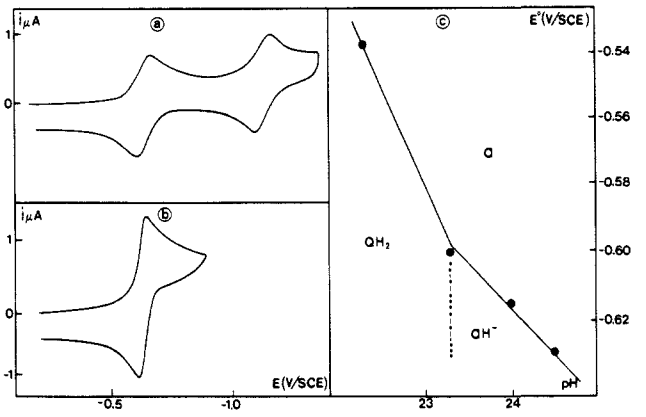

Figure 9. Cyclic voltammetry of 0.2 mM 1,4-naphthoquinone in acetonitrile +0.1 M NEt_4BF_4 at 20 °C at a platinum 2 mm diameter electrode in the absence of acid (a) and in the presence of a 8.8 mM phenol/1.2 mM phenate buffer (b). (c) Potential pH diagram of the 1,4-naphthoquinone/1,4-dihydroxynaphthalene couple.

spite of a plateau value being 3–4 orders of magnitude below the diffusion limit. The pK_a was then determined as the pH corresponding to the intersection of these two linear portions of the plot. In fact, the low pH rising linear section of the plot has a slope (0.39) much smaller than 1, clearly indicating that the forward and backward reactions are under activation control. The intersection between the two linear portions of the plot thus does not correspond to the pK_a of the $AH^{\bullet+}/A^{\bullet}$ couple, but is located, as are all the experimental data points, in a substantially exergonic region of the deprotonation reaction.

Experimental Section

Reagents. All pyridines used were commercially available. 10-Methylacridan and 10-methylacridinium iodide were prepared according to a previously published procedure.[22] The solution were prepared with acetonitrile (Merck Uvasol) and deoxygenated with argon before use. Tetraethylammonium tetrafluoroborate (Fluka, puriss) was used as supporting electrolyte.

Apparatus and Procedures. The ultramicroelectrodes were prepared by sealing gold or platinum wires (Goodfellow Metal Ltd.) according to a previously described procedure.[8a] The reference electrode was an aqueous SCE and the counterelectrode a platinum grid. The cell was placed in a Faraday cage. The potentiostat with a three-electron configuration was the same as previously described.[8,23] Chronoamperograms and voltammograms were recorded with a Nicolet 4094C/4180 (8 bits, 5-ns sampling time) digital oscilloscope. The function generator was an Enertec 4431. In double potential step experiments, the current–time curves were repeated 10 times and accumulated before transfer into an IBM PC-AT microcomputer for treatment.[9b] The whole set of measurements was repeated again 10 times. Under these conditions, the dispersion in the measurement of R was found to be less than 0.05. A 17-μm gold electrode was used for times θ between 24 μs and 1 ms, and a 5-μm gold electrode for time θ between 3 to 50 μs.[9b] In linear sweep voltammetry experiments, each curve was repeated 10 times and accumulated in the digital oscilloscope. The values of i_p (peak in presence of bases) and i_{p0} (peak current is absence of bases) were measured directly at the same electrode with the same solution, by subtracting the base line.[24] The dispersion error on the value of the ratio i_p/i_{p0} was found to be less than 0.15. Experimental absorption spectra were obtained with a Varian Superscan 3 UV–visible spectrophotometer. The reactions were carried out at 20 °C under nitrogen atmosphere and the spectra were recorded from aliquots diluted 20 times. $E°_{Q/QH_2}$ was determined as follows. In an 8.8 mM phenol/1.2 mM phenate buffer (pH = 24.5[16a]); Q (0.2 mM) gives rise to a single two-electron reversible cyclic voltammogram (30 mV between cathodic and anodic peaks) at 0.1 $V \cdot s^{-1}$ (Figure 9). The standard potential, measured as the midpoint between the cathodic and anodic peak is then −0.630 V vs SCE. Upon raising the pH the single two-electron wave splits into two waves, whereas upon decreasing the pH it loses its reversibility. Zero-current potentiometric measurements were also carried out in acetic/acetate buffers at pH = 24, 23.3, and 23.3.[16b] At pH 24, an $E°$ value of −0.615 V vs SCE was obtained almost instantaneously, whereas stable values of −0.600 and −0.540 V vs SCE were obtained at pH 23.3 and 22.3 after 10- and 60-min equilibration periods, respectively. The resulting $E°$ – pH plot (Figure 9b) thus shows two regions with 29 and 58 mV slopes corresponding to the $Q/QH^{\bullet-}$ and Q/QH_2 couples, respectively. The value of $E°_{Q/QH_2}$ ensues.[25]

(22) Roberts, R. M. G.; Ostovic, D.; Kreevoy, M. M. *Faraday Discuss. Chem. Soc.* **1982**, *74*, 257.

(23) Garreau, D.; Hapiot, P.; Savéant, J.-M. *J. Electroanal. Chem.* **1989**, *272*, 1.

(24) The effects of ohmic drop, mutual influence of the ohmic drop and capacitive current,[8a] and heterogeneous electron-transfer kinetics[7a] on the ratio i_p/i_{p0} were checked to be negligible in our working conditions.

(25) And thus the value of the pK_a of the QH_2/QH^- couple is 23.3 (±0.3).

Evidence for Lifetime Distributions in Cyclodextrin Inclusion Complexes

Frank V. Bright,* Gino C. Catena, and Jingfan Huang

Contribution from the Department of Chemistry, Acheson Hall, State University of New York at Buffalo, Buffalo, New York 14214. *Received July 24, 1989*

Abstract: Multifrequency phase and modulation fluorescence spectroscopy are used to study 1:1 inclusion complexes of β-cyclodextrin (βCD) with several anilinonaphthalene sulfonate (ANS) probes. Our time-resolved fluorescence results indicate that the inclusion complex is described most accurately by distributed fluorescence lifetime models. This indicates that the ANS probe is not in a single discrete environment within the cyclodextrin cavity but in an array of cyclodextrin-cavity environments all in equilibrium with one another.

Cyclodextrins (CD's) are toroidally shaped polysaccharides made up of six to eight D-glucose monomers.[1] The CD cavities are hydrophobic and have internal diameters ranging from 4.7–8.3 Å.[2] Because of the size and hydrophobic nature of CD's they form inclusion complexes with many small molecules.[1,2] As a result, CD's have been used extnesively to model protein–ligand and enzyme–substrate interactions,[3] have found widespread ap-

* Author to whom all correspondence should be directed.

(1) See, for example: (a) Baeyens, W. R. G.; Ling, B. L.; De Moerloose, P.; Del Castillo, B.; De Jonge, C. *Ann. Rev. Acad. Farm.* **1988**, *54*, 698. (b) *Inclusion Compounds*; Atwood, J. L., Davis, J. E. D., Mac Nicol, D. D., Eds.; Academic Press: London, 1984; Vol. 2 and 3.

0002-7863/90/1512-1343$02.50/0

plication in the separation sciences,[4] and have been used for selective synthetic strategies.[5]

Over the years, numerous instrumental techniques have been employed to investigate the CD inclusion process.[6-14] For example, both spectral and temporal fluorometric techniques have been utilized to study the thermodynamics[2,10] and kinetics[11-13] of fluorescent probes included within CD cavities. In the course of these studies, investigators learned that nearly all CD inclusion complexes were either 1:1, 1:2, or 2:2 (probe:cyclodextrin) in nature. Recent electron spin resonance (ESR) spectroscopic studies have shown, however, that even simple 1:1 complexes can be more complicated than at first glance.[14,15] Specifically, when α-phenyl-2,4,6-trimethoxybenzyl *tert*-butyl nitroxide (aminoxyl) and various *tert*-butyl nitroxides are included by γ-cyclodextrin, two unique (discrete) 1:1 inclusion complexes are formed. The two complexes form with the phenyl or *tert*-butyl groups included within the cyclodextrin cavity.[14] It was shown that these two 1:1 complexes have formation constants that differ by between a factor three and five depending on the particular substituents. While these ESR results are interesting and quite compelling, it is not at all clear if a particular inclusion complex (e.g., 1:1) is itself a discrete entity or an average of several forms of the same 1:1 inclusion complex in different stages of complexation.

In this report we present results of nanosecond time-resolved fluorescence experiments on four substituted anilinonaphthalene sulfonates (ANS) included by β-cyclodextrin (βCD). These compounds (**1–4**; inclusates) were chosen primarily because they form simple 1:1 inclusion complexes with βCD.[10] We analyze our experimental data with classical discrete decay law models and recently developed distribution analysis techniques.[16] Our experimental data are clearly best described by a unimodal Gaussian or Lorentzian distribution of fluorescence lifetimes which is consistent with ANS coexisting in several βCD environments. That is, there is not a single 1:1 inclusion complex but an ensemble of 1:1 inclusion complexes all in equilibrium with one another.

Theory

Multiexponential Decays. The time course of fluorescence intensity ($I(t)$) decays are usually described as a sum of discrete exponentials:

$$I(t) = \Sigma\alpha_i \exp(-t/\tau_i) \tag{1}$$

where τ_i and α_i are the individual fluorescence lifetimes and associated preexponential factors for the ith component, respectively. The fractional contribution of the ith component to the total fluorescence is given by

$$F_i = \alpha_i\tau_i/\Sigma\alpha_i\tau_i \tag{2}$$

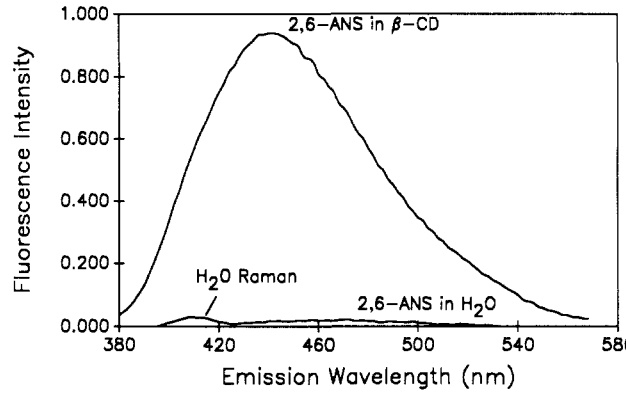

Figure 1. Steady-state emission spectra for 10 μM 2,6-ANS with and without 10 mM βCD.

where $\Sigma F_i = 1$.

Lifetime Distributions. Consider the model in which the amplitude of the preexponetial factors are described by a continuous distribution (i.e., $\alpha(\tau)$). The time course of the intensity decay now contains components of the lifetime and $\alpha(\tau)$ given by

$$I(\tau,t) = \alpha(\tau) \exp(-t/\tau) \tag{3}$$

The corresponding total decay is

$$I(t) = \int \alpha(\tau) \exp(-t/\tau)\, dt \tag{4}$$

where $\int\alpha(\tau)d\tau = 1$. In the present work, Gaussian (G) and Lorentzian (L) distributions were used to describe $\alpha(\tau)$. Specifically, the $\alpha(\tau)$ functions are

$$\alpha_G(\tau) = 1/\sigma\sqrt{2\pi} \exp[-0.5((\tau - \tau')/\sigma)^2] \tag{5}$$

$$\alpha_L(\tau) = 1/\pi \exp[H/((\tau - \tau')^2 + H^2] \tag{6}$$

where τ' is the central value of the lifetime distribution, σ is the standard deviation of the Gaussian, and H is the half-width at half-maximum (HWHM) for the Lorentzian. By using the functional forms for $\alpha(\tau)$ we minimize the number of floating parameters in our fit model. For example, by using a unimodal Lorentzian distribution (eq 6) one has only two floating parameters (τ' and H) compared to three for a double exponential discrete decay law. The more complex multimodal lifetime distributions have been presented in the literature.[16]

In frequency-domain fluorescence spectroscopy, the measured quantities are the frequency-dependent (ω) phase shift ($\Phi(\omega)_m$) and demodulation factor ($M(\omega)_m$). For any assumed decay model these values can be calculated from the sine ($S(\omega)$) and cosine ($C(\omega)$) Fourier transforms of the impulse-response function:

$$S(\omega) = \int_{\tau=0}^{\infty} \frac{\alpha(\tau)\omega\tau^2}{1 + \omega^2\tau^2}\, d\tau \Big/ \int_{\tau=0}^{\infty} \alpha(\tau)\tau\, d\tau \tag{7}$$

$$C(\omega) = \int_{\tau=0}^{\infty} \frac{\alpha(\tau)\tau}{1 + \omega^2\tau^2} d\tau \Big/ \int_{\tau=0}^{\infty} \alpha(\tau)\tau\, d\tau \tag{8}$$

For any set of parameters the calculated phase and modulation are given by

$$\Phi(\omega)_c = \arctan\,(S(\omega)/C(\omega)) \tag{9}$$

$$M(\omega)_c = (S(\omega)^2 + C(\omega)^2)^{1/2} \tag{10}$$

The decay parameters of interest (τ, ($\alpha(\tau)$, etc.) are recovered from the experimental data by the method of nonlinear least squares.[17] We judge the goodness-of-fit by the reduced χ^2

$$\chi^2 = \frac{1}{\nu}\left\{\sum_{\omega}\left(\frac{\Phi(\omega)_m - \Phi(\omega)_c}{\sigma_\Phi}\right)^2 + \sum_{\omega}\left(\frac{M(\omega)_m - M(\omega)_c}{\sigma_m}\right)^2\right\} \tag{11}$$

(2) Saenger, W. *Angew. Chem., Int. Ed. Engl.* **1980**, *19*, 344.
(3) Bender, M. L.; Komiyama, M. *Cyclodextrin Chemistry*; Springer-Verlag: Berlin, 1978.
(4) Armstrong, D. W.; Alak, A.; Bui, K.; De Mond, W.; Ward, T.; Riehl, T. E. *J. Inclusion Phenom.* **1984**, *2*, 533.
(5) Ihara, Y.; Nakanishi, E.; Nango, M.; Koga, J. *J. Bull. Chem. Soc. Jpn.* **1986**, *59*, 1901.
(6) Schlenk, H.; Sand, D. M. *J. Am. Chem. Soc.* **1961**, *83*, 2312.
(7) Laufer, D. A.; Johnson, R. F.; Fuhrman, H. S.; Cardelino, B.; Schwartz, L. M.; Gelb, R. I. *J. Am. Chem. Soc.* **1981**, *103*, 1750.
(8) Ross, J. B. A.; Orstan, A. *J. Phys. Chem.* **1987**, *91*, 2739.
(9) Turro, N. J.; Cox, G. S. *Photochem. Photobiol.* **1984**, *40*, 185.
(10) Catena, G. C.; Bright, F. V. *Anal. Chem.* **1989**, *61*, 905.
(11) Hersey, A.; Robinson, B. H.; Kelly, H. C. *J. Chem. Soc., Faraday Trans. 1* **1986**, *82*, 1271.
(12) Kitamura, S.; Matsumori, S.; Kuge, T. *J. Inclusion Phenom.* **1984**, *2*, 725.
(13) Jobe, D. J.; Verrall, R. E.; Palepu, R.; Reinsborough, V. C. *J. Phys. Chem.* **1988**, *92*, 3582.
(14) Kotake, Y.; Janzen, E. G. *J. Am. Chem. Soc.* **1989**, *111*, 5138.
(15) Kotake, Y.; Janzen, E. G. *J. Am. Chem. Soc.* **1988**, *110*, 3699.
(16) See, for example: (a) Alcala, J. R.; Gratton, E.; Prendergast, F. G. *Biophys. J.* **1987**, *51*, 587. (b) Alcala, J. R.; Gratton, E.; Prendergast, F. G. *Biophys. J.* **1987**, *51*, 597. (c) Alcala, J. R.; Gratton, E.; Prendergast, F. G. *Biophys. J.* **1987**, *51*, 925. (d) Eftink, M. R.; Wasylewski, Z. *Biochemistry* **1989**, *28*, 382. (e) James, D. R.; Liu, Y.-S. De Mayo, P.; Ware, W. R. *Chem. Phys. Lett.* **1985**, *120*, 460. (f) Lakowicz, J. R.; Gryczynski, I.; Cheung, H. C.; Wang, C.-K.; Johnson, M. L.; Joshi, N. *Biochemistry* **1988**, *27*, 9149. (g) Gryczynski, I.; Wiczk, W.; Johnson, M. L.; Cheung, H. C.; Wang, C.-K.; Lakowicz, J. R. *Biophys. J.* **1988**, *54*, 577.

Table I. Results for Nonlinear Least-Squares Fits of Multifrequency Phase Angle and Demodulation Factor Data to Various Decay Law Models

	inclusate			
model[a]	2,6-ANS	2,7-ANS	2,8-ANS	1,8-ANS
		Single		
T1	5.38	8.67	6.35	1.74
X^2	6.11	17.8	592	995
		Double		
T1	6.52	9.55	8.70	2.82
T2	3.59	3.62	3.69	0.94
F1	0.53	0.90	0.69	0.64
X^2	10.5	4.99	7.68	17.2
		Gaussian		
T1	5.58	9.10	7.21	2.11
W	1.13	2.52	2.62	1.14
X^2	1.38	1.07	1.10	1.23
		Lorentzian		
T1	5.55	8.99	6.92	1.92
W	0.85	2.02	2.86	1.50
X^2	1.40	1.06	0.89	1.16

[a] T1, fluorescence lifetime for component 1 (ns); T2, fluorescence lifetime for component 2 (ns); F1, fractional contribution to lifetime component 1; X^2, χ-squared value; W, standard deviation for Gaussian and half width at half maximum for Lorentzian distribution.

where υ is the number of degrees of freedom,[18] and $\sigma_\Phi = 0.15°$ and $\sigma_M = 0.002$ are the uncertainties in the measured phase angle and demodulation factor values, respectively. If the assumed uncertainties truly reflect the uncertainty in the data, then an ideal fit will yield a χ^2 value of unity.

Results and Discussion

Figure 1 shows a typical pair of steady-state emission spectra for 10 μM 2,6-ANS (**1**) in the presence and absence of 10 mM βCD. Clearly, the presence of βCD results in a dramatic increase in the total fluorescence intensity. Under our experimental conditions the free fluorescent probes (**1**–**4**) contribute ≤3%

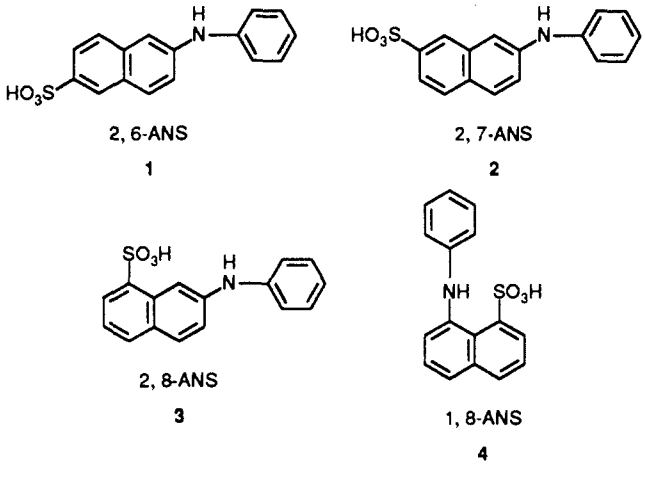

compared to their βCD-complexed forms. In addition to an increase in intensity, we observe a hypsochromic shift in the emission spectra. This is a result of the fluorescent probe being selectively included into the more hydrophobic environment of the βCD cavity compared to the solvent water.

(17) See, for example: (a) Lakowicz, J. R.; Gratton, E.; Lacko, G.; Cherek, H.; Limkemann, M. *Biophys. J.* **1984**, *46*, 463. (b) Gratton, E.; Lakowicz, J. R.; Maliwal, B.; Cherek, H.; Lacko, G.; Limkemann, M. *Biophys. J.* **1984**, *46*, 479.

(18) For our experiments υ is typically 25–40.

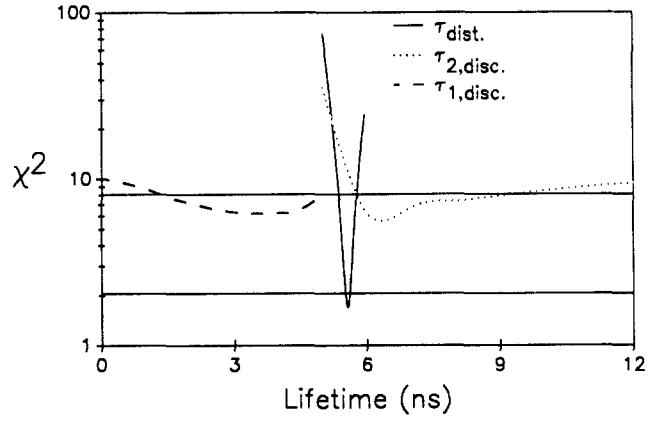

Figure 2. Lifetime confidence intervals (χ^2 versus lifetime) for a unimodal Gaussian distribution (—) and the double discrete decay model (– –, ···) fit to 2,6-ANS included in βCD. The upper and lower vertical solid lines denote one standard deviation above the χ^2 minima for the discrete and distributed decay models, respectively.

Table I summarizes the results of nonlinear least-squares[19] fits of our experimental data to several decay law models. In all cases, these results show that the single and double discrete lifetime models poorly describe the experimental data. This is indicated best by the nonunity χ^2 value. Further support for dismissing the discrete decay law models come from the following: (1) the large and often systematic deviations within the residual errors (not shown); (2) a poor correlation between steady-state and time-resolved experimental results (vide infra); and (3) inordinately broad confidence interval (χ^2 vs lifetime) curves (Figure 2).

Under our experimental conditions, uncomplexed (free) ANS contributes ≤3% to the total steady-state signal compared to complexed ANS (Figure 1). However, the double exponential lifetime model (Table I) continually recovers a value far in excess of 3%, in poor agreement with the steady-state experiment. Moreover, the lifetime recovered from the discrete double exponential fit (Table I), corresponding to free ANS (see below), is always larger than for free ANS determined from separate experiments (<400 ps).

Figure 2 shows the lifetime confidence intervals (χ^2 versus recovered lifetime) for a unimodal Gaussian and discrete double exponential fits to the 2,6-ANS data. To construct these curves the lifetime being investigated is fixed at a given value (x-axis), and the χ^2 is minimized with the remaining parameters floated. By using this approach any correlation between fit parameters is accounted for. The upper and lower horizontal lines correspond to one standard deviation above the χ^2 minima for the discrete and distributed models, respectively. Clearly, the unimodal Gaussian fit results in a very narrow confidence interval (i.e., a small uncertainty) of about 150 ps. In contrast, the uncertainties in the recovered discrete lifetime values are several nanoseconds. This is another good indication that the discrete model is incorrect since the Gaussian model contains fewer floating parameters, compared to the double exponential, but gives a superior fit and significantly lower (by at least a factor of 10) uncertainties in the fit parameters.

Of course, there is the very real possibility that two distinct 1:1 complexes exist for the ANS–βCD system. This could potentially result in two distinct fluorescent lifetimes. However, our earlier work in this area[10] has shown that the inclusion complexation of these particular ANS probes with βCD are well-described by only one formation constant (K_f). In addition, we showed evidence for the 1:1 complex forming over the naphthalene moiety in opposition to the benzene ring.[10] In contrast, a probe like 2-(*p*-toluidinyl)naphthalene-6-sulfonic acid (**5**, 2,6-TNS) exhibits 1:1 and 2:1 (CD:ANS) complexation.[10,13] This is striking

(19) Beechem, J. M.; Gratton, E. *Proc. SPIE* **1988**, *909*, 70.

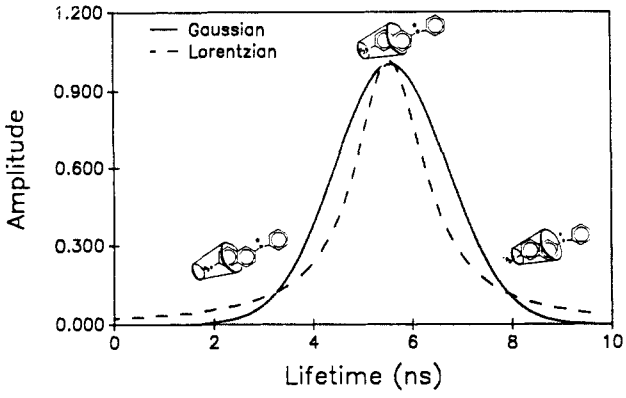

Figure 3. Recovered unimodal Gaussian (—) and Lorentzian (- -) lifetime distributions for 10^{-5} M 2,6-ANS in 10 mM BCD at 25 °C. The inclusion complex structures represent possible conformations responsible for the lifetime distribution process.

considering that the only difference between 2,6-ANS (**1**) and 2,6-TNS (**5**) is the substitution of a methyl group in the para

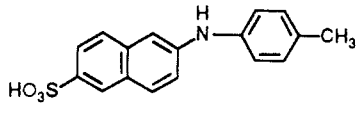

2, 6-TNS

5

position of the benzene ring. This methyl substitution results in the clear appearance of a 1:1 (K_f = 1980 L/mol) and a 2:1 (K_f = 600 L/mol) complex.[10] Considering this, we find it hard to believe two distinct 1:1 complexes could form for our particular ANS–βCD systems, one over the naphthalene and another over benzene moieties, not be observed, have similar formation constants, and still exhibit *significantly* different lifetimes. Moreover, it is even more inconceivable that two types of the 1:1 complex would have the same enthalpy and entropy.[10] In summary, if the second apparent fluorescence lifetime were to truly reflect the formation of a second form of the 1:1 complex, we believe the relative strength of this complex should be different enough to have allowed us to observe it in our earlier work.[10] To date, we have not seen any evidence to support the formation of this second 1:1 species.

Thus, we conclude that the nanosecond decay kinetics of ANS–βCD inclusion complexes are modeled most accurately by either Gaussian or Lorentzian lifetime distributions. At present we are not able to distinguish between Gaussian or Lorentzian models because the χ^2 values are too similar. However, experience tells us that Lorentzian distribution models usually fit better than Gaussian models because the wings of the Lorentzian allow more for imprecision in the experimental data.

Figure 3 presents recovered unimodal Gaussian and Lorentzian distributions for the 2,6-ANS–βCD inclusion complex. In addition to the two curves, we illustrate several 2,6-ANS–βCD conformations that we propose dominate at each point along the lifetime distributions. In the short lifetime regime, the distributions are dominated by a 2,6-ANS–βCD complex that is not fully formed. The ANS is partially free from the βCD and thus accessible to and collisionally quenched by the solvent water. In contrast, at the longer lifetime edge the inclusion complex is formed fully with 2,6-ANS buried as far as possible into the βCD cavity. The probe is protected from the solvent to the greatest extent allowed, and the fluorescence lifetime concomitantly increases. Finally, at intermediate points on the distribution curves 2,6-ANS is in intermediate states of inclusion neither totally buried nor free in the solvent.

Summarizing, we present experimental evidence supporting our contention that ANS probes included by βCD are described accurately by a distributed lifetime process. In turn, this indicates that there is an ensemble of similarly formed ANS–βCD complexes all in coexistence with each other.

In the future, we plan to explore the impact of these observations on the thermodynamics of ANS–βCD complexes, investigate how such distributions influence internal cyclodextrin cavity local viscosities, determine the effects of quenchers on the recovered distributions, and study the effects of distributed decay times on the recovered rotational dynamics of ANS–βCD complexes.

Experimental Section

Sample Preparation. All samples used for study were prepared in 0.10 M, pH 7.00 phosphate buffer. Distilled, deionized water was used throughout to prepare all stock solutions. For all results reported here the ANS and βCD concentrations are 10^{-5} M and 10 mM, respectively. At these levels, all samples were free of primary and secondary interfilter effects. Inert gases were not used to remove dissolved oxygen.

Materials. β-Cyclodextrin was purchased from Sigma Chemical Company and used without further purification. The background signal from 10 mM β-cyclodextrin was ≤0.25% of the total fluorescence. 2-Anilinonaphthalene-6-sulfonic acid (**1**; 2,6-ANS), 2-anilinonaphthalene-7-sulfonic acid (**2**; 2,7-ANS), 2-anilinonaphthalene-8-sulfonic acid (**3**; 2,8-ANS), and 1-anilinonaphthalene-8-sulfonic acid (**4**; 1,8-ANS) were obtained from Molecular Probes. The purity of each was checked by reversed-phase HPLC, and each was found to contain no discernable impurities at an absorbance of 364 nm.

Fluorescence Lifetime Measurements. Samples for study were prepared fresh daily and run immediately after preparation. We found that "older" samples yielded very complex decay kinetics. Reproducible experimental results were routinely obtained for samples run within 6 h or for those that were kept refrigerated for up to 5 days. All sample measurements were made with the use of quartz cuvettes. The instrumentation used for these measurements has been described in detail elsewhere.[20] For all results reported laser excitation is at 363.8 nm, fluorescence is monitored through a 420-nm longpass filter (Oriel), and magic angle polarization is used for all measurements.[21] The reference lifetime standard for all these experiments is Me_2POPOP in ethanol with a lifetime of 1.45 ns.[22]

Acknowledgment. This work was supported by BRSG S07 RR 07066 awarded by the Biomedical Research Support Grant Program, Division of Resources, National Institutes of Health, the donors of the Petroleum Research Fund, administered by the American Chemical Society, a New Faculty Development Award from the New York State/United University Professions, a Non-Tenured Faculty Grant from 3M, Inc., the Health Care Instruments and Devices Institute at SUNY-Buffalo, and the National Institute of Mental Health.

(20) Bright, F. V. *Anal. Chem.* **1988**, *60*, 1622.
(21) Spencer, R. D.; Weber, G. *J. Chem. Phys.* **1970**, *52*, 1654.
(22) Lakowicz, J. R.; Cherek, H.; Balter, A. *J. Biochem. Biophys. Methods* **1981**, *5*, 131.